JCTC Journal of Chemical Theory and Computation

How Is cis−trans Isomerization Controlled in Dronpa Mutants? A Replica Exchange Molecular Dynamics Study

Samuel L. C. Moors, Servaas Michielssens, Cristina Flors,† Peter Dedecker, Johan Hofkens, and Arnout Ceulemans*

Department of Chemistry and INPAC Institute for Nanoscale Physics and Chemistry, K. U. Leuven, Leuven, Belgium

Received February 1, 2008

Abstract: The reversibly photoactivatable green fluorescent protein analog Dronpa holds great promise as a marker for various new cellular imaging applications. Using a replica exchange method which combines both Hamiltonian and temperature exchanges, the ground-state dynamics of Dronpa and two mutants with increased switching kinetics, Val157Gly and Met159Thr, were compared. The dominant chromophore state was found to be the cis isomer in all three proteins. The simulation data suggest that both mutations strongly increase the chromophore flexibility and cis−trans isomerization rate. We identify three key amino acids, Val157, Met159, and Phe173, which are able to impede the bottom hula-twist transition path, depending on their position and rotameric state. We believe our insights will help to understand the switching process and provide useful information for the design of new variants with improved fluorescence properties.

Introduction

Dronpa, a monomeric mutant of a fluorescent protein from the coral *Pectiniidae Echinophyllia* sp. SC22, sharing 81% sequence identity with the fluorescent protein KikG from the coral *Favia favus*, emits 518 nm light with a high fluorescence quantum yield ($\Phi_{FL} = 0.85$).[1,2] At neutral or basic pH, Dronpa can be photoswitched from a bright (fluorescent) state to a dark (nonfluorescent) state by intense 488 nm light. The photoswitched dark state has a half-lifetime of 14 h.[3] Illumination with 405 nm light efficiently switches the dark state back to the bright state. This on−off switching process is highly reversible (>100 cycles),[4] opening up a host of new applications including dynamic optical labeling and tracking of proteins, organelles, or cells and detection of protein interactions using high-resolution imaging.[5,6]

Recently, through semirandom mutagenesis, Ando et al. discovered two Dronpa mutants, Dronpa Met159Thr (Dronpa-2) and Dronpa Val157Ile/Met159Ala (Dronpa-3), which display increased photoinduced and spontaneous switching kinetics.[7] Compared to Dronpa, both mutants can be turned off more efficiently with 488 nm light and returned more quickly to their emissive states in the dark but have much lower fluorescence quantum yields ($\Phi_{FL} = 0.33$ and 0.28 respectively). Ensemble and single-molecule fluorescence experiments suggested increased conformational freedom of the chromophore in Dronpa-2 and Dronpa-3 and formation of a dark intermediate state arising from cis−trans isomerization.[8] Independently, Stiel et al.[3] also discovered Dronpa-2, together with another fast-switching mutant, Dronpa Val157Gly (rsFastLime), with a slightly decreased fluorescence quantum yield ($\Phi_{FL} = 0.77$). Both variants were designed by structural comparison of Dronpa with asFP595 from the sea anemone *Anemonia sulcata*. Like Dronpa, asFP595 is a reversibly photoactivatable protein. With only four differing residues, the immediate chromophore environments of asFP595 and Dronpa are very similar. Unlike the Dronpa chromophore, which adopts a fluorescent cis conformation, the equilibrated asFP595 chromophore is in a nonfluorescent trans conformation. The residues Val157 and Ser142 in Dronpa are replaced in asFP595 at the equivalent positions by serine and alanine, respectively. As a result, the favorable H-bond between the cis chromophore and

* Corresponding author tel.: (32)16/32.73.63; fax: (32)16/32.79.92; e-mail: Arnout.Ceulemans@chem.kuleuven.be.

† Present address: School of Chemistry, University of Edinburgh, UK.

10.1021/ct8000359 CCC: $40.75
Published on Web 05/20/2008

Ser142 in Dronpa is replaced by an H-bond between the trans chromophore and Ser157 in asFP595. The spectroscopic properties of asFP595 are also different from Dronpa. Upon photoactivation with 540−560 nm light, the asFP595 chromophore isomerizes to a cis coplanar state, which is converted back to the nonfluorescent trans state, either thermally or by illumination with 450 nm light.[9,10] By modeling a trans chromophore into the cis X-ray structure of Dronpa, Stiel et al. suggested that mutations at Val157 and Met159 reduce the steric hindrance for a similar cis−trans isomerization in Dronpa.[3] Remarkably, all three mutants, Dronpa-2, Dronpa-3, and rsFastLime, arise from the replacement of only Val157 or Met159, or both.

X-ray diffraction of bright-state Dronpa crystals, which were photoswitched to the dark state and subsequently flash-frozen in liquid nitrogen to trap the chromophore in its dark state conformation, showed that cis-to-trans isomerization did indeed occur, accompanied by structural rearrangements of several nearby amino acid residues.[11] The transition mechanism however remains largely speculative. Upon photobleaching, the anionic chromophore of Dronpa is protonated at the phenolate oxygen to the neutral state.[1] The switching process is further complicated by the existence of several dark intermediate states and an excited-state proton transfer reaction.[4,12]

To gain deeper insight in the dynamics of the electronic ground state at the molecular level, we investigated the cis−trans equilibrium distributions and transition paths in solution of Dronpa, rsFastLime, and Dronpa-2 using a replica exchange method which combines exchanges between replicas with different Hamiltonians and temperatures (HT-REM). Both Dronpa mutants display increased chromophore flexibility and lower cis−trans isomerization barriers. Our simulations point out three key residues, Val157, Met159, and Phe173, which control the isomerization process. Substitution of Val157 to Gly greatly increases the conformational freedom of the chromophore by allowing a Phe173 shift away from the chromophore and a consequent reshuffling of the Met159 rotamer population. Replacement of the bulky Met159 with the smaller threonine elevates the steric hindrance with the chromophore in the cis state and along the hula-twist isomerization pathway and allows the chromophore to shift toward the protein surface, which decreases the stability of the trans state by steric hindrance with Val157.

Methods

Force Field Parameters. The chromophore force field parameters for both the anionic and neutral forms were modeled from quantum chemical calculations using Gaussian 03.[13] The atomic charges were determined with the RED program,[14] which automates the optimization of the molecular electrostatic potential and the restricted electrostatic potential charges from HF/6-31G* calculations on 4′-hydroxybenzylidene-2,3-dimethyl-imidazolinone (HBDI; Figure 1), compatible with the Amber force field. The dihedral angle parameters for φ and τ were fitted from B3LYP/6-31G* calculations on HBDI at various φ and τ angles. Using the dihedral energy term $E_{\text{dihedral}} = k_\varphi[1 + \cos(n\varphi - \varphi_0)]$,

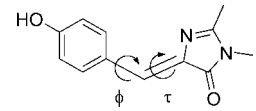

Figure 1. Structure of HBDI, used as a model for the calculation of the neutral chromophore force field parameters. For the anionic chromophore, the phenolate form of HBDI was used.

we obtained force constants $k_\varphi = 3.015$ kcal mol^{-1} and $k_\tau = 3.900$ kcal mol^{-1} and $k_\phi = 1.185$ kcal mol^{-1} and $k_\tau = 5.900$ kcal mol^{-1} for the anionic and neutral chromophores, respectively, which leads to total energy barriers $\Delta U_\varphi = 24.120$ kcal mol^{-1} and $\Delta U_\tau = 31.200$ kcal mol^{-1} and $\Delta U_\varphi = 9.480$ kcal mol^{-1} and $\Delta U_\tau = 47.200$ kcal mol^{-1} for the anionic and neutral chromophores, respectively. Similar values were obtained by Reuter et al.: $k_\varphi = 2.700$ kcal mol^{-1} and $k_\tau = 3.900$ kcal mol^{-1} and $k_\varphi = 1.400$ kcal mol^{-1} and $k_\tau = 6.840$ kcal mol^{-1} for the anionic and neutral chromophores, respectively.[15] The remaining parameters were obtained from analogues' functional groups already present in the Amber force field. A complete list of the chromophore parameters and charges can be found in the Supporting Information.

Molecular Dynamics Simulations. All molecular dynamics (MD) simulations were started from the bright-state X-ray structure of Dronpa (Protein Databank (PDB) code 2IE2), which was mutated at the relevant positions with the Swiss-PdbViewer.[16] The Amber 2003 force field[17] was used with a modified version of the Amber 8 software.[18] The smooth particle mesh Ewald method[19] was employed to accommodate long-range electrostatic forces. The nonbonded cutoff for van der Waals interactions was set to 8 Å. Covalent bonds involving hydrogen atoms were constrained using SHAKE.[20] A time step of 2 fs was used. Samples were collected every 0.5 ps. The temperature was controlled using the Berendsen weak-coupling algorithm.[21] The His193 pyrrole was protonated. The charged protein, with crystallographic waters included, was neutralized with sodium ions and solvated in a truncated octahedral TIP3P[22] water box, which extended the system with at least 8 Å at each side of the box. After rotating the chromophore to the trans isomer and mutation of the relevant residues, the system was minimized and equilibrated for 2.5 ns at 300 K and 1 bar.

Hamiltonian and Temperature Replica Exchange. To overcome the cis−trans energy barrier, normally not accessible using conventional MD, a combined Hamiltonian[23] and temperature[24,25] REM (HT-REM) simulation was performed. The exchange probability P_{acc} between two replicas i and j with reduced coordinates X_i and X_j, reciprocal temperatures β_i and β_j, and differing potential energy functions $U_i(X)$ and $U_j(X)$ is given as

$$P_{\text{acc}}(i,j) = \min\{1, \exp[\beta_i(U_i(X_i) - U_i(X_j)) - \beta_j(U_j(X_i) - U_j(X_j))]\} \quad (1)$$

Exchanges were attempted between replicas with differing temperature and force field parameters. A total of 20 replicas were distributed evenly over the 300−350.5 K temperature range, while gradually lowering the φ and τ force constants

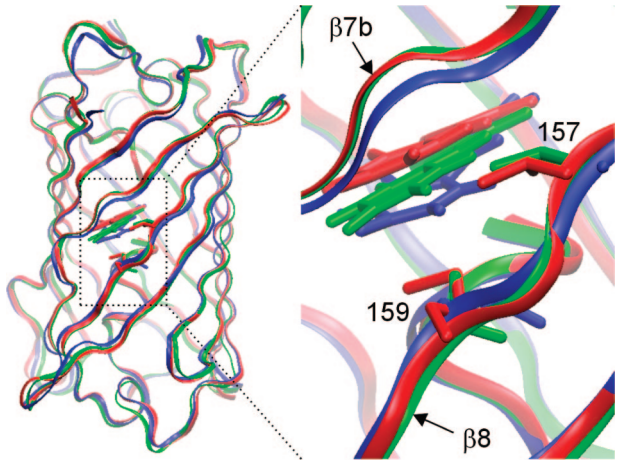

Figure 2. Ribbon diagrams of neutral Dronpa (red), rsFastLime (blue), and Dronpa-2 (green), with the chromophore and respective residues in positions 157 and 159. Each structure was generated by taking the average over 20 random snapshots. Compared to Dronpa, strand β7b is located closer to strand β8, while the Dronpa-2 chromophore is shifted towards the solvent.

to zero at 350.5 K. In the highest temperature replica, where the φ and τ dihedral terms are removed, the intrinsic potential surface of the chromophore displays minima at φ and τ angles of approximately +90°/−90°, about 2.5 kcal mol^{-1} lower than the coplanar conformation. This inverted surface enhances the sampling of the cis−trans transition state. Note that the inverted rotational barriers are much lower than the calculated barriers for HBDI. The time constant for temperature coupling was 0.5 ps. Exchanges were attempted every 0.5 ps. Acceptance probabilities between neighboring temperatures varied between 0.19 and 0.27. After each successful exchange, all velocities were randomly reassigned from a Maxwell−Boltzmann distribution. The HT-REM simulation was carried out for 37.5 ns per replica, the last 12.5 ns of which were used to calculate the reported thermodynamic properties. For Dronpa-2, 25 ns per replica were simulated, the last 12.5 ns of which were used. The following criteria for H-bond interaction were taken: the distance between the donor (D) and acceptor (A) must be smaller than 3.3 Å, and the D−H−A angle must be larger than 120°. Standard errors of the thermodynamic averages were calculated using the statistical inefficiency method.[26] Free energy plots were calculated using a multistate Bennett acceptance ratio implementation, which is suitable for the analysis of multiple simulations conducted under arbitrary conditions.[27,28]

Results and Discussion

Secondary Structure. HT-REM simulations were performed on Dronpa, rsFastLime, and Dronpa-2 with the chromophore in its neutral form as well as on the anionic form of rsFastLime. A total of 20 replicas were distributed evenly over the 300−350.5 K temperature range, with concomitant gradual lowering of the φ and τ force constants to zero at 350.5 K. As shown in Figure 2, in all simulations, the β-barrel secondary structure is very similar. The average backbone root-mean-square deviations from the Dronpa X-ray structue are around 1.1 Å. The cleft between strands β7 and β10, which was highlighted by Stiel et al.,[3] is preserved in all simulations and provides a dynamic water bridge between the chromophore and the bulk solvent. This cleft originates from a kink in strand β7 at Pro141, which divides the strand into two parts, β7a and β7b. Interestingly, the β7 kink also causes a disruption of the H-bonding pattern between strands β7b and β8, from Pro141 to Thr143, close to the chromophore phenol moiety (Figure 2). In rsFastLime, the backbone distance between strands β7b and β8 is significantly reduced; the average distance between the Thr143 O and the Asn158 N reduces from 5.3 Å in Dronpa to 4.5 Å, effectively filling up the space that arises from Val157Gly mutation. In Dronpa-2, no such adjustment of secondary structure was observed. Instead, the freed space from replacing the bulky methionine by threonine is partly filled by the chromophore, which is shifted toward the protein surface; the distance between the chromophore phenol oxygen and Glu140 O reduces by 0.3 Å. As a result, the phenol ring is more exposed to the solvent (via the cleft) and the degree of H-bonding with a nearby water molecule is increased from 4% in Dronpa to 33% in Dronpa-2.

cis−trans Equilibria. The equilibrium distributions of the chromophore and several rotational isomeric states of surrounding residues are listed in Table 1. All HT-REM simulations started from a sample in which the chromophore had been equilibrated for 2.5 ns in the trans state. In Figure 3, the equilibration of the trans chromophore population over time is shown. In neutral Dronpa-2, the trans population rapidly decreases to zero after 6 ns. Also in anionic rsFastLime, the trans population gradually fades away. In contrast, a small fraction of trans remains for the neutral forms of rsFastLime (5%) and Dronpa (2%). Irradiation with 405 nm light of thermally equilibrated rsFastLime resulted in a 2-fold increase of fluorescence.[3] Thus, there must be a nonfluorescent state with 50% population or a less fluorescent state with even higher population. Since a trans population of at most 5% is found in rsFastLime, our results indicate that trans-to-cis isomerization alone cannot explain this 2-fold fluorescence increase. As an alternative, a neutral cis state could be responsible for the residual dark state population in thermal equilibrium.

The increased stability of the trans isomer in the neutral chromophore compared to the anionic chromophore can be explained by a favorable H-bond interaction of the phenolate oxygen with the Ser142 hydroxy group (Figure 4). In rsFastLime, the anionic cis chromophore is indeed more tightly H-bonded with Ser142 than the neutral chromophore (75% H-bond population versus 20%, respectively). In Dronpa-2, the stability of the trans state is very low compared to the cis state (*vide infra*). The chromophore shift toward Glu140 O (see above) causes steric hindrance with Val157 in the trans conformation. Additionally, the cis state is stabilized by reduced steric interactions of the cis chromophore with Thr159 in Dronpa-2 in comparison with Met159 in Dronpa.

Along with cis−trans isomerization, several surrounding residues undergo significant displacement. The Phe173 side chain appears to play a central role. Contrary to all available

Table 1. Populations of Chromophore Isomer States and Several Surrounding Residue Rotamer States

		cis				
rotational isomeric state		Dronpa (X-ray)[a]	Dronpa (neutral)	Dronpa-2 (neutral)	rsFastLime (neutral)	rsFastLime (anionic)
chromophore τ	0°	1	0.98 ± 0.01	1	0.95 ± 0.02	1
Phe173 χ1	180°	0	0.007 ± 0.004	0.10 ± 0.02	0.02 ± 0.01	0
	+60°	0	0.72 ± 0.03	0.84 ± 0.03	0.94 ± 0.02	0.83 ± 0.03
	−60°	1	0.28 ± 0.03	0.05 ± 0.03	0.04 ± 0.01	0.17 ± 0.03
Met159/Thr159 χ1	180°	0.0	0	0.45 ± 0.04	0	0.01 ± 0.01
	+60°	0	0.55 ± 0.04	0.51 ± 0.04	0.86 ± 0.04	0.53 ± 0.05
	−60°	1	0.45 ± 0.04	0.03 ± 0.01	0.14 ± 0.04	0.47 ± 0.04
Val157 χ1	180°	0.2	0.28 ± 0.05	0.37 ± 0.03		
	+60°	0.8	0.72 ± 0.05	0.62 ± 0.03		
	−60°	0	0	0		
Ser142 χ1	180°	0	0.64 ± 0.03	0.42 ± 0.04	0.22 ± 0.06	0.16 ± 0.05
	+60°	1	0.02 ± 0.01	0.12 ± 0.02	0.36 ± 0.10	0.69 ± 0.07
	−60°	0	0.34 ± 0.03	0.46 ± 0.04	0.41 ± 0.07	0.16 ± 0.05

		trans				
rotational isomeric state		Dronpa (X-ray)[b]	Dronpa (neutral)	Dronpa-2 (neutral)	rsFastLime (neutral)	rsFastLime (anionic)
chromophore τ	180°	1	0.02 ± 0.01	0	0.05 ± 0.02	0
Phe173 χ1	180°	0	0		0	
	+60°	0	0		0	
	−60°	1	1		1	
Met159/Thr159 χ1	180°	0	0		0.06 ± 0.03	
	+60°	0	0.69 ± 0.17		0.53 ± 0.09	
	−60°	1	0.31 ± 0.17		0.42 ± 0.09	
Val157 χ1	180°	0	0			
	+60°	1	1			
	−60°	0	0			
Ser142 χ1	180°	0.5	0.41 ± 0.12		0.4 ± 0.2	
	+60°	0.5	0.59 ± 0.12		0.5 ± 0.2	
	−60°	0	0		0.06 ± 0.03	

[a] Average values taken from all chains of PDB X-ray structures 2IE2, 2IOV, and 2GX0. [b] Average values taken from all chains of PDB X-ray structure 2POX.

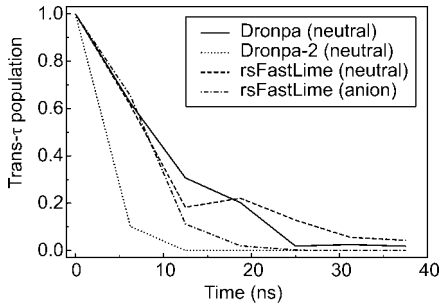

Figure 3. Evolution of the trans chromophore population at 300 K as a function of simulation time.

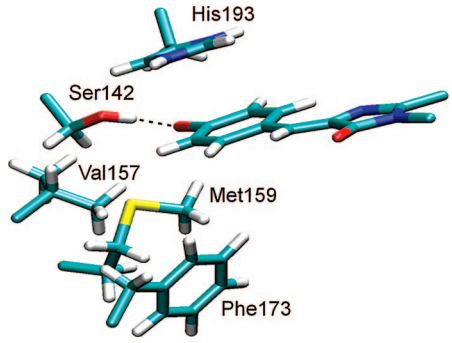

Figure 4. X-ray structure of the anionic Dronpa chromophore, H-bonded with Ser142, and surrounding residues.

Dronpa X-ray structures, in all simulated proteins, the Phe173 χ1 dihedral is mostly in its +60° rotameric state (Table 1), the phenyl ring leaning toward residue 157. This difference between the MD predicted rotamers in solution and the X-ray data is possibly due to packing effects in the crystal structure. Note that, in the Dronpa crystal structures, the Phe173 χ2 dihedral considerably deviates from its ideal 90° angle (χ2 = 19−44°). In both neutral Dronpa and rsFastLime simulations, Phe173 χ1 undergoes a rotamer shift from +60° in cis to −60° in trans, due to a steric clash between the trans chromophore and the Phe173 χ1 (=+60°) rotamer (Figure 5a). In rsFastLime, Met159 χ1 is correlated with Phe173 χ1. Steric hindrance with the Phe173 χ1 (=+60°) state restricts Met159 χ1 in the +60° rotamer, while in the Phe173 χ1 (= −60°) state, Met159 χ1 is about equally distributed over +60° and −60° (Figure 5b). In Dronpa, this correlation is not apparent. Steric interaction with the Val157 isopropyl group in *cis*-Dronpa moves the Phe173 χ1 (= +60°) phenyl ring away from Met159 CG, allowing Met159 χ1 to occupy both +60° and −60°.

In anionic rsFastLime, Ser142 is mainly positioned toward the chromophore with χ1 = +60° (Table 1), in agreement with the X-ray structure of bright-state Dronpa. In the protein with the neutral chromophore, however, Ser142 χ1 is distributed over the three rotamers, in accordance with the dark-state X-ray structure of Dronpa,[11] which exhibits a disordered Ser142 residue (χ1 = −164°/69°). In the χ1 = −60° rotamer, the Ser142 hydroxy group is H-bonded with the Glu140 carbonyl oxygen, whereas in the χ1 = 180° rotamer, a H-bond is formed with the Asn155 carbonyl

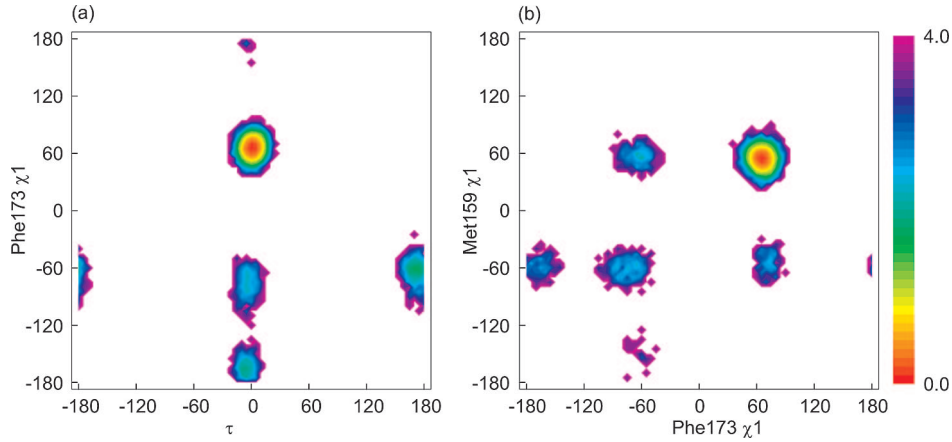

Figure 5. Free energy as a function of (a) τ and Phe173 χ1 and (b) Phe173 χ1 and Met159 χ1, from rsFastLime (neutral chromophore) samples at 300 K in kcal mol^{-1}. Values of τ equal to 0° and 180° correspond to the cis and trans isomers respectively.

Table 2. Chromophore Deviation From Planarity[a]

	cis			trans		
	τ (deg)	φ (deg)	θ (deg)	τ (deg)	φ (deg)	θ (deg)
Dronpa (X-ray)	1.5[b]/12.5[c]/1.1[d]	−6.9[b]/−17.4[c]/−0.3[d]	7.6[b]/13.4[c]/2.1[d]	160.5[e]	36.3[e]	26.7[e]
Dronpa (neutral)	0.3(6.1)	−7.1(5.9)	10.0(5.5)	181.1(6.8)	−10.0(7.4)	17.9(8.7)
Dronpa-2 (neutral)	2.1(6.0)	−3.3(10.5)	10.4(5.9)			
rsFastLime (neutral)	0.4(6.6)	−16.2(13.0)	19.8(10.5)	171.7(6.8)	−25.8(11.1)	35.8(8.5)
rsFastLime (anion)	3.0(7.0)	−4.6(9.2)	11.6(6.2)			
Chromo (neutral)[f]	−0.07(7.0)	−0.5(17.0)	16.2(9.3)			

[a] Average values of θ were calculated as the angle (in degrees) between the planes formed by the atoms C_9, C_{10}, and N_1 and C_{11}, C_{14}, and C_{15}. Standard deviations are given between parentheses. [b] PDB X-ray data are average angles over all chains taken from 2IE2. [c] PDB X-ray data are average angles over all chains taken from 2IOV. [d] PDB X-ray data are average angles over all chains taken from 2GX0. [e] PDB X-ray data are average angles over all chains taken from 2POX. [f] Data extracted from a 6 ns HT-REM simulation of the neutral chromophore in water under identical conditions as the proteins (not shown).

oxygen. This result also supports the hypothesis that the trans and cis chromophore states are neutral and anionic, respectively. Like in the dark-state X-ray structure, Val157 changes its position toward the solvent to accommodate the new conformation of the chromophore phenol ring.[11] However, the structural rearrangements of His193 and Arg66 in the dark-state X-ray structure were not observed in any of our simulations at 300 K. Note that the trans X-ray structure does not represent a fully relaxed conformation, since it was formed upon irradiation of the Dronpa molecules within the solid crystal, which strongly limits the dynamics of the protein. In contrast, the simulations that we performed allowed for full relaxation of the trans form in solution at 300 K. Specifically in the highest-temperature simulations, both His193 and Arg66 side groups undergo frequent rotamer transitions, suggesting that the absence of His193 and Arg66 rotamers at 300 K is *not* due to insufficient sampling.

In our simulations, we have only considered the anionic and neutral chromophore. The 390 and 503 nm absorption maxima of Dronpa, which correspond respectively to the neutral and anionic states of the phenolic hydroxyl of the chromophore,[1] are similar to those of other green fluorescent protein mutants. Hybrid quantum-classical calculations of the equilibria between the different protonation states of the solvated chromophore (cation, neutral, zwitterion, and anion) indicated that, at neutral pH, only the neutral and anionic states are populated in the ground state.[29] This suggests that a zwitterionic or cationic state can only exist if the protonated imidazolinone ring is sufficiently stabilized by the surrounding protein matrix. In the X-ray structure of asFP595, where a zwitterionic chromophore state has been proposed,[30] protonation of the imidazolinone nitrogen is stabilized by a H-bond with the nearby Glu215. In both cis and trans X-ray structures of Dronpa, no such stabilizing H-bond can be formed. These data suggest that the neutral and anionic chromophores are the most important ground states in Dronpa, although the existence of a zwitterionic or cationic intermediate state cannot be excluded.

Chromophore Flexibility. In both cis and trans isomers of the free chromophore in the ground state, the phenol and imidazolidone rings adopt a coplanar conformation.[31] The angle θ between the planes of the two rings is determined by φ and τ. At 300 K, θ mostly correlates with rotation about φ. Table 2 lists the average τ, φ, and θ values and standard deviations for the simulated proteins. For both rsFastLime and Dronpa, the average θ value in trans is much higher than in cis, in agreement with the X-ray structures of cis and trans Dronpa. In rsFastLime, the deviation from planarity and flexibility are much higher for the neutral than for the anionic protein, due to the higher φ force constant k_φ for anionic rsFastLime.

Compared to Dronpa and Dronpa-2, the average value and standard deviation of θ in rsFastLime are twice as high. In rsFastLime, the Thr59 methyl group collides with the chromophore phenol from below at one side, causing rotation

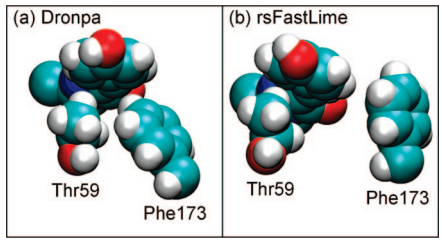

Figure 6. van der Waals representation of the chromophore in interaction with residues Thr59 and Phe173. (a) In Dronpa, φ rotation is largely offset by steric effects with Phe173, which is pushed toward the chromophore by Val157. (b) In rsFastLime, collision with Thr59 on the side of the chromophore phenol causes a disruption of coplanarity by φ rotation.

of the φ dihedral (Figure 6b). van der Waals interactions with Val157 in Dronpa cause the Phe173 phenyl ring to shift considerably toward the chromophore. As a result, the Phe173 phenyl ring is also positioned below the chromophore phenol ring, preventing large φ deviations (Figure 6a).

The cis−trans Transition Pathway. To investigate the isomerization pathways of the electronic ground state, we calculated the unbiased free energy as a function of τ and φ, on the basis of all replicas (Figure 7). For all simulated proteins, the cis-to-trans transition starts by concerted rotation of both φ and τ, the bridging methine group rotating up toward His193 and the phenol group pointing down. This so-called bottom hula-twist pathway minimizes the motion of the chromophore phenol ring and its surroundings. However, once the transition state ($\tau \sim 90°$) is crossed, the pathway becomes less defined. In addition to continuing the hula-twist path, the φ dihedral may also rotate back to its starting angle. This alternative pathway is possible thanks to the increased rotational freedom of the phenol ring around φ in the trans state. Simulations by Andresen et al.[10] on asFP595 suggested that the chromophore undergoes a trans−cis isomerization through a similar bottom hula-twist mechanism. Using force probe MD, the nonequilibrium photoisomerization process was simulated by shifting the φ and τ dihedral potentials over a short time scale. The HT-REM scheme used in this work, however, does not force the chromophore in any direction. Instead, in the highest temperature replica, the φ and τ potentials are completely removed, and the cis−trans transition path is determined solely by the surrounding protein matrix.

Despite limited sampling of the transition state, barriers of isomerization for both rsFastLime (neutral and anonic) and Dronpa-2 appear lower compared to Dronpa (Figure 7). For rsFastLime (neutral and anionic), cis−trans isomerization is hindered when Phe173 or Met159 or both are in the −60° χ1 rotameric state (Figure 8). Before trans-to-cis transition takes place, Phe173 χ1 and Met159 χ1 undergo a −60° to +60° rotamer shift. In Dronpa, sampling of the transition region is very low; isomerization is hindered by both Phe173 χ1 conformations −60° and +60°. Thus, we conclude that Val157 affects the transition barrier indirectly through both Phe173 and Met159.

In Dronpa-2, trans conformations are infrequently sampled and only in the highest temperature replicas (Figure 7c). As a result of the increased free energy of the trans state, the trans-to-cis barrier is drastically lowered, which correlates well with the strongly increased thermal recovery rate of the Dronpa-2 bright state compared to Dronpa.[3,7] Full rotation to the trans isomer is prevented by steric interaction of the phenol oxygen with the Val157 side chain. Since τ remains below 160°, Phe173 χ1 stays mainly in its +60° rotameric state, favorable for cis−trans isomerization. Also, no change in the Thr159 χ1 rotamer distribution was observed in the transition region.

Remarkably, the anionic chromophore of rsFastLime remains H-bonded to Ser142 from the cis state to well past the transition state region ($\tau \sim -30°$ to +120°). Considering the increased stability of the H-bonded chromophore, this suggests that the neutral trans chromophore deprotonates before returning to the cis state. Indeed, Fron et al.[12] compared the transient absorption properties of deuterated and nondeuterated Dronpa samples and found that exited-state proton transfer is involved in the first step of the off-to-on photoconversion, which takes place within a 4 ps time frame.

Comparing the calculated free energy barriers of Dronpa and Dronpa-2 with those obtained from fluorescence experiments (26.0 kcal mol^{-1} and 7.2 kcal mol^{-1}, respectively[8,32]), we find that the calculated barriers are much higher. Possible explanations for this difference are (i) overestimated dihedral force field parameters for φ and τ, (ii) neglect of polarization effects of the surrounding residues on the chromophore,[33] (iii) insufficient sampling of the transition state region, or (iv) involvement of a photoswitching process which does not depend on cis−trans isomerization.

Fluorescence Quantum Yield. Several sources of fluorescence quantum yield loss in fluorescent proteins have been suggested in the literature, most notably excited-state rotation about τ (twisting) with subsequent fast internal conversion, which is accelerated by increased chromophore flexibility or noncoplanarity.[34–37] Excited state quenching with molecular oxygen[38] or with water molecules through H-bonding[39] has also been proposed.

When Dronpa and its mutants are compared, the fluorescence quantum yield and switching rates appear highly correlated. As shown in Figure 7, the free energy basin of the cis state of rsFastLime and Dronpa-2 is considerably broadened toward the hula-twist transition state in comparison with Dronpa. This increased conformational freedom of τ might at least partially explain the reduced fluorescence quantum yield of rsFastLime and Dronpa-2. In rsFastLime, the high average value and standard deviation of θ in the cis state (Table 2) could also accelerate internal conversion. In Dronpa-2, the chromophore shift toward the protein surface causes increased solvent accessibility and H-bonding with nearby water molecules, which may well account for the additional reduction of the fluorescence quantum yield in Dronpa-2. Assuming that the photoswitched off state is trans, the high nonplanarity of the trans state of Dronpa and

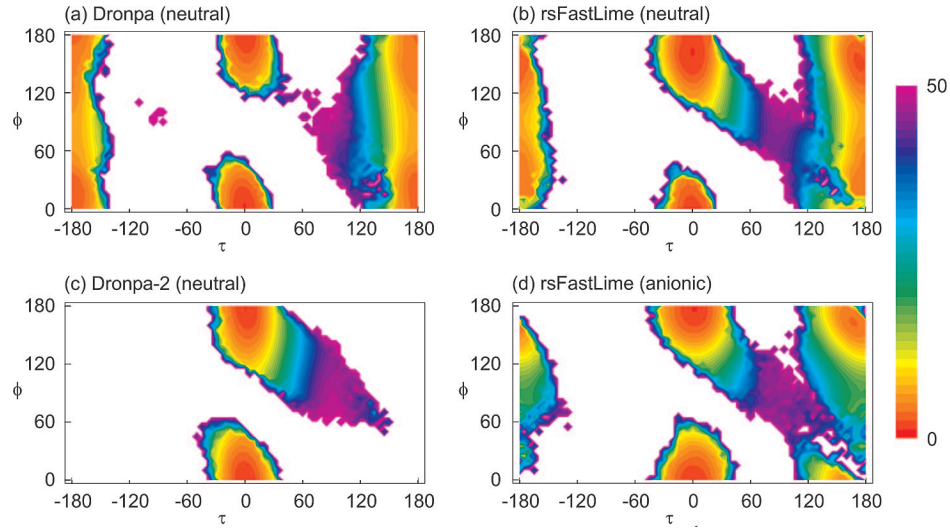

Figure 7. Unbiased free energy as a function of τ and φ in kcal mol^{-1}. (a) Dronpa with neutral chromophore (cis-to-trans free energy barrier $\Delta G^{\ddagger} = 50$ kcal mol^{-1}). (b) rsFastLime with neutral chromophore ($\Delta G^{\ddagger} = 45$ kcal mol^{-1}). (c) Dronpa-2 with neutral chromophore ($\Delta G^{\ddagger} = 46$ kcal mol^{-1}). (d) rsFastLime with anionic chromophore ($\Delta G^{\ddagger} = 45$ kcal mol^{-1}).

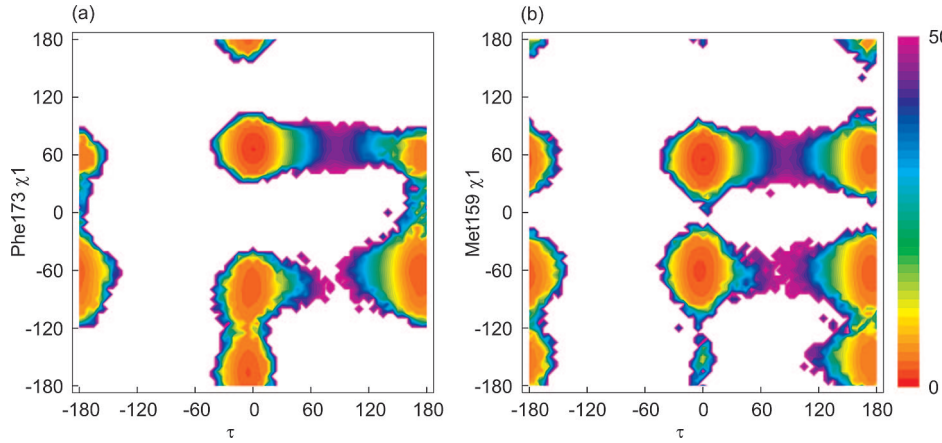

Figure 8. Unbiased free energy as a function of (a) τ and Phe173 χ1 and (b) τ and Met159 χ1, from rsFastLime (neutral chromophore) in kcal mol^{-1}.

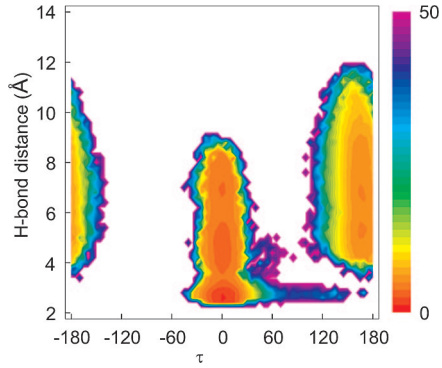

Figure 9. Unbiased free energy as a function of τ and the H-bond distance between the chromophore phenolate oxygen and Ser142 carbonyl oxygen from rsFastLime (anionic chromophore) in kcal mol^{-1}.

rsFastLime (Table 2) could be responsible for the very weak fluorescence of the photoswitched off state.

Conclusion

Canonical HT-REM simulations on the native state show that three residues, Val157, Met159, and Phe173, play a key role in the cis−trans equilibrium and bottom hula-twist transition path of Dronpa and mutants. In rsFastLime, cis−trans transition is most favorable when Phe173 and Met159 χ1 are in the +60° rotameric states. Compared to rsFastLime, the increased isomerization free energy barrier in Dronpa is attributed to steric interactions of the chromophore with the Phe173 χ1 (= +60°) rotamer in the transition state, due in turn to steric interactions of Phe173 with Val157, which cause a displacement of the Phe173 phenyl ring toward the chromophore. In comparison with Dronpa, the Dronpa-2 isomerization free energy barrier is lowered by replacement of the bulky Met159 by Thr159. The cis chromophore isomer predominated in all simulated proteins. The Dronpa-2 trans state is strongly destabilized by steric interaction of the chromophore with Val157, causing a drastic reduction of the trans-to-cis barrier. While so far mutagenic studies have only pointed to the relevance of Val157 and Met159, the present study draws attention to Phe173 as a third residue, which may strongly influence photoswitching. Subsequent study will be focused on further

increasing the photoinduced and spontaneous switching kinetics of Dronpa and variants.

Acknowledgment. We thank John Chodera (University of California, San Francisco) for providing a preview of ref 27 and kind assistance with the calculation of the unbiased free energy plots from the HT-REM simulations. This work was financially supported by the "Fonds voor Wetenschappelijk Onderzoek − Vlaanderen". P.D. is a fellow of the FWO (aspirant van het FWO). This research was conducted utilizing high-performance computational resources provided by the University of Leuven (http://ludit.kuleuven.be/hpc).

Supporting Information Available: Chromophore charges and parameters compatible with the Amber force field. This material is available free of charge via the Internet at http://pubs.acs.org.

References

(1) Ando, R.; Mizuno, H.; Miyawaki, A. Regulated fast nucleocytoplasmic shuttling observed by reversible protein highlighting. *Science* **2004**, *306* (5700), 1370–1373.

(2) Wilmann, P. G.; Turcic, K.; Battad, J. M.; Wilce, M. C. J.; Devenish, R. J.; Prescott, M.; Rossjohn, J. The 1.7 angstrom crystal structure of Dronpa: A photoswitchable green fluorescent protein. *J. Mol. Biol.* **2006**, *364* (2), 213–224.

(3) Stiel, A. C.; Trowitzsch, S.; Weber, G.; Andresen, M.; Eggeling, C.; Hell, S. W.; Jakobs, S.; Wahl, M. C. 1.8 angstrom bright-state structure of the reversibly switchable fluorescent protein Dronpa guides the generation of fast switching variants. *Biochem. J.* **2007**, *402*, 35–42.

(4) Habuchi, S.; Ando, R.; Dedecker, P.; Verheijen, W.; Mizuno, H.; Miyawaki, A.; Hofkens, J. Reversible single-molecule photoswitching in the GFP-like fluorescent protein Dronpa. *Proc. Natl. Acad. Sci. U.S.A.* **2005**, *102* (27), 9511–9516.

(5) Dedecker, P.; Hotta, J. I.; Flors, C.; Sliwa, M.; Uji, I. H.; Roeffaers, M. B. J.; Ando, R.; Mizuno, H.; Miyawaki, A.; Hofkens, J. Subdiffraction imaging through the selective donut-mode depletion of thermally stable photoswitchable fluorophores: Numerical analysis and application to the fluorescent protein Dronpa. *J. Am. Chem. Soc.* **2007**, *129* (51), 16132–16141.

(6) Lukyanov, K. A.; Chudakov, D. M.; Lukyanov, S.; Verkhusha, V. V. Photoactivatable fluorescent proteins. *Nat. Rev. Mol. Cell Biol.* **2005**, *6* (11), 885–891.

(7) Ando, R.; Flors, C.; Mizuno, H.; Hofkens, J.; Miyawaki, A. Highlighted generation of fluorescence signals using simultaneous two-color irradiation on Dronpa mutants. *Biophys. J.* **2007**, *92* (12), L97–L99.

(8) Flors, C.; Hotta, J. I.; Uji, I. H.; Dedecker, P.; Ando, R.; Mizuno, H.; Miyawaki, A.; Hofkens, J. A Stroboscopic Approach for Fast Photoactivation-Localization Microscopy with Dronpa Mutants. *J. Am. Chem. Soc.* **2007**, *129* (45), 13970–13977.

(9) Chudakov, D. M.; Feofanov, A. V.; Mudriku, N. N.; Lukyanov, S.; Lukyanov, K. A. Chromophore environment provides clue to "kindling fluorescent protein" riddle. *J. Biol. Chem.* **2003**, *278* (9), 7215–7219.

(10) Andresen, M.; Wahl, M. C.; Stiel, A. C.; Grater, F.; Schafer, L. V.; Trowitzsch, S.; Weber, G.; Eggeling, C.; Grubmuller, H.; Hell, S. W.; Jakobs, S. Structure and mechanism of the reversible photoswitch of a fluorescent protein. *Proc. Natl. Acad. Sci. U.S.A.* **2005**, *102* (37), 13070–13074.

(11) Andresen, M.; Stiel, A. C.; Trowitzsch, S.; Weber, G.; Eggeling, C.; Wahl, M. C.; Hell, S. W.; Jakobs, S. Structural basis for reversible photoswitching in Dronpa. *Proc. Natl. Acad. Sci. U.S.A.* **2007**, *104* (32), 13005–13009.

(12) Fron, E.; Flors, C.; Schweitzer, G.; Habuchi, S.; Mizuno, H.; Ando, R.; De Schryver, F. C.; Miyawaki, A.; Hofkens, J. Ultrafast excited-state dynamics of the photoswitchable protein dronpa. *J. Am. Chem. Soc.* **2007**, *129* (16), 4870–4871.

(13) Frisch, M. J. et al. *Gaussian 03*, revision C.02; Gaussian, Inc.: Wallingford CT, 2004.

(14) Pigache, A.; Cieplak, P.; Dupradeau, F. Y. Automatic and highly reproducible RESP and ESP charge derivation: Application to the development of programs RED and X RED. *Abstr. Pap.—Am. Chem. Soc.* **2004**, *227*, U1011–U1011.

(15) Reuter, N.; Lin, R.; Thiel, W. Green fluorescent proteins: Empirical force field for the neutral and deprotonated forms of the chromophore. Molecular dynamics simulation's of the wild type and S65T mutant. *J. Phys. Chem. B* **2002**, *106* (24), 6310–6321.

(16) Guex, N.; Peitsch, M. C. SWISS-MODEL and the Swiss-PdbViewer: An environment for comparative protein modeling. *Electrophoresis* **1997**, *18* (15), 2714–2723.

(17) Duan, Y.; Wu, C.; Chowdhury, S.; Lee, M. C.; Xiong, G. M.; Zhang, W.; Yang, R.; Cieplak, P.; Luo, R.; Lee, T.; Caldwell, J.; Wang, J. M.; Kollman, P. A point-charge force field for molecular mechanics simulations of proteins based on condensed-phase quantum mechanical calculations. *J. Comput. Chem.* **2003**, *24* (16), 1999–2012.

(18) Case, D. A.; Darden, T. A.; Cheatham, T. E., III; Simmerling, C. L.; Wang, J.; Duke, R. E.; Luo, R.; Merz, K. M.; Wang, B.; Pearlman, D. A.; Crowley, M.; Brozell, S.; Tsui, V.; Gohlke, H.; Mongan, J.; Hornak, V.; Cui, G.; Beroza, P.; Schafmeister, C.; Caldwell, J. W.; Ross, W. S.; Kollman, P. A. *AMBER 8*; University of California: San Francisco, 2004.

(19) Essmann, U.; Perera, L.; Berkowitz, M. L.; Darden, T.; Lee, H.; Pedersen, L. G. A Smooth Particle Mesh Ewald Method. *J. Chem. Phys.* **1995**, *103* (19), 8577–8593.

(20) Ryckaert, J.-P.; Ciccotti, G.; Berendsen, H. J. C. Numerical integration of the cartesian equations of motion of a system with constraints: Molecular dynamics of n-alkanes. *J. Comput. Phys.* **1977**, *23*, 327–341.

(21) Berendsen, H. J. C.; Postma, J. P. M.; Vangunsteren, W. F.; Dinola, A.; Haak, J. R. Molecular-Dynamics with Coupling to an External Bath. *J. Chem. Phys.* **1984**, *81* (8), 3684–3690.

(22) Jorgensen, W. L.; Chandrasekhar, J.; Madura, J. D.; Impey, R. W.; Klein, M. L. Comparison of Simple Potential Functions for Simulating Liquid Water. *J. Chem. Phys.* **1983**, *79* (2), 926–935.

(23) Fukunishi, H.; Watanabe, O.; Takada, S. On the Hamiltonian replica exchange method for efficient sampling of biomolecular systems: Application to protein structure prediction. *J. Chem. Phys.* **2002**, *116* (20), 9058–9067.

(24) Sugita, Y.; Okamoto, Y. Replica-exchange molecular dynamics method for protein folding. *Chem. Phys. Lett.* **1999**, *314* (1−2), 141–151.

(25) Moors, S. L. C.; Hellings, M.; De Maeyer, M.; Engelborghs, Y.; Ceulemans, A. Tryptophan rotamers as evidenced by X-ray, fluorescence lifetimes, and molecular dynamics modeling. *Biophys. J.* **2006**, *91* (3), 816–823.

(26) Allen, M. P.; Tildesley, D. J. *Computer Simulation of Liquids*; Oxford University Press: New York, 1987.

(27) Shirts, M. R.; Chodera, J. D. Statistically optimal analysis of samples from multiple equilibrium states. arXiv:0801.1426v2 [physics.comp-ph] 2008.

(28) Maragakis, P.; Spichty, M.; Karplus, M. Optimal estimates of free energies from multistate nonequilibrium work data. *Phys. Rev. Lett.* **2006**, *96* (10), 100602.

(29) Scharnagl, C.; Raupp-Kossmann, R. A. Solution pK(a) values of the green fluorescent protein chromophore from hybrid quantum-classical calculations. *J. Phys. Chem. B* **2004**, *108* (1), 477–489.

(30) Schafer, L. V.; Groenhof, G.; Klingen, A. R.; Ullmann, G. M.; Boggio-Pasqua, M.; Robb, M. A.; Grubmuller, H. Photoswitching of the fluorescent protein asFP595: Mechanism, proton pathways, and absorption spectra. *Angew. Chem., Int. Ed.* **2007**, *46* (4), 530–536.

(31) Weber, W.; Helms, V.; McCammon, J. A.; Langhoff, P. W. Shedding light on the dark and weakly fluorescent states of green fluorescent proteins. *Proc. Natl. Acad. Sci. U.S.A.* **1999**, *96* (11), 6177–6182.

(32) Habuchi, S.; Dedecker, P.; Hotta, J. I.; Flors, C.; Ando, R.; Mizuno, H.; Miyawaki, A.; Hofkens, J. Photo-induced protonation/deprotonation in the GFP-like fluorescent protein Dronpa: mechanism responsible for the reversible photoswitching. *Photochem. Photobiol. Sci.* **2006**, *5* (6), 567–576.

(33) He, X.; Bell, A. F.; Tonge, P. J. Ground state isomerization of a model green fluorescent protein chromophore. *FEBS Lett.* **2003**, *549* (1−3), 35–38.

(34) Altoe, P.; Bernardi, F.; Garavelli, M.; Orlandi, G.; Negri, F. Solvent effects on the vibrational activity and photodynamics of the green fluorescent protein chromophore: A quantum-chemical study. *J. Am. Chem. Soc.* **2005**, *127* (11), 3952–3963.

(35) Mandal, D.; Tahara, T.; Meech, S. R. Excited-state dynamics in the green fluorescent protein chromophore. *J. Phys. Chem. B* **2004**, *108* (3), 1102–1108.

(36) Litvinenko, K. L.; Webber, N. M.; Meech, S. R. Internal conversion in the chromophore of the green fluorescent protein: Temperature dependence and isoviscosity analysis. *J. Phys. Chem. A* **2003**, *107* (15), 2616–2623.

(37) Wilmann, P. G.; Petersen, J.; Pettikiriarachchi, A.; Buckle, A. M.; Smith, S. C.; Olsen, S.; Perugini, M. A.; Devenish, R. J.; Prescott, M.; Rossjohn, J. The 2.1 angstrom crystal structure of the far-red fluorescent protein HcRed: Inherent conformational flexibility of the chromophore. *J. Mol. Biol.* **2005**, *349* (1), 223–237.

(38) Brejc, K.; Sixma, T. K.; Kitts, P. A.; Kain, S. R.; Tsien, R. Y.; Ormo, M.; Remington, S. J. Structural basis for dual excitation and photoisomerization of the Aequorea victoria green fluorescent protein. *Proc. Natl. Acad. Sci. U.S.A.* **1997**, *94* (6), 2306–2311.

(39) Follenius-Wund, A.; Bourotte, M.; Schmitt, M.; Iyice, F.; Lami, H.; Bourguignon, J. J.; Haiech, J.; Pigault, C. Fluorescent derivatives of the GFP chromophore give a new insight into the GFP fluorescence process. *Biophys. J.* **2003**, *85* (3), 1839–1850.

CT8000359